Articles

Synthesis and Characterization of New Symmetrical Binucleating Ligands and Their μ-Phenoxo-Bridged Bicopper(II) Complexes: Structural, Electrochemical, and Magnetic Studies

P. Amudha and M. Kandaswamy*

Department of Inorganic Chemistry, School of Chemical Sciences, University of Madras,
Guindy Campus, Chennai-25, India

L. Govindasamy and D. Velmurugan

Department of Crystallography and Biophysics, University of Madras, Guindy Campus,
Chennai-25, India

Received November 26, 1997

The new pentadentate binucleating ligands 2,6-Bis[*N*-(3,5-dimethyl-2-hydroxybenzyl)-*N*-methylaminomethyl]-4-chlorophenol, H_3L^1, and 2,6-bis[*N*-(3,5-dichloro-2-hydroxybenzyl)-*N*-cyclohexylaminomethyl]-4-methylphenol, H_3L^2, and their binuclear copper(II) complexes of the general formulas $[Cu_2L^1(X)]$ (X = OMe, OH, Br (**1**−**3**)) and $[Cu_2L^2(X)]$ (X = OMe, OH, Br (**4**−**6**)) have been prepared. The molecular structure of the complex $[Cu_2L^1(OMe)]\cdot MeOH$ was studied by X-ray crystallography. It exists as a discrete binuclear species in which the copper atoms are in a distorted square planar environment with two oxygen bridges provided by the phenolate of the ligand and methoxy exogenous donor and the Cu···Cu distance is 3.030 Å. A cyclic voltammetric study of the complexes shows two quasireversible reduction waves at negative potentials. A cryomagnetic investigation on powdered samples of the complexes (**1**−**6**) shows moderately strong antiferromagnetic coupling ($-2J$ in the range 120−300 cm^{-1}). A comparison of the electrochemical and magnetic properties of the complexes prepared from both ligands is discussed. Crystal data for the complex $[Cu_2L^1(OMe)]\cdot MeOH$: molecular formula $C_{30}H_{39}ClCu_2N_2O_5$, monoclinic, space group $P2_1/c$ with $a = 13.222(1)$ Å, $b = 15.912(1)$ Å, $c = 14.149(1)$ Å, $\beta = 91.64(1)°$, and $Z = 4$.

Introduction

Interest in the synthesis of new binuclear copper(II) complexes is due to their applications in bioinorganic chemistry and their physicochemical aspects. Involvement of one or more metal ions in various complex biological processes is well established.[1] The binuclear copper core is found in several metalloproteins, such as hemocyanin (dioxygen carriers), tyrosinase (hydroxylation of phenols to catechols and subsequent oxidation of diphenols to quinones), laccase (oxidation of diphenols to quinones), ceruloplasmin (Fe and Cu transport in blood serum), etc.[2] Although they undertake various functions, they do have similar chemical properties at the bicopper active site, such as antiferromagnetism, EPR inactivity, and the ability to transfer two or more electrons reversibly and simultaneously at positive potentials.

Complexity due to their hugh size makes it difficult to understand the exact structure and functions of these proteins. As an attempt toward this goal, several researchers have synthesized wide varieties of small binuclear copper complexes as models for these metalloproteins and studied their properties on the basis of the spectral, electrochemical, and magnetic behaviors of these model complexes.[3] These studies offered additional information about the mechanism of exchange interaction between the paramagnetic metal centers which is useful in finding appropriate building units for the construction of new magnetic materials[4] and in the development of new redox catalysts for reactions other than biologically important ones.

Binuclear copper(II) complexes with endogenous phenolic bridges so far reported have been prepared from the ligands obtained by following the standard procedures using 2,6-

---

(1) Fenton, D. E. In *Advances in Inorganic and Bioinorganic Mechanisms*; Skyes, A. G., Ed.; Academic: London, 1983; Vol. 2, p 187.

(2) (a) Karlin, K. D.; Zubieta, J. *Biological and Inorganic Copper Chemistry*; Academic: New York, 1996. (b) *Bioinorganic Chemistry of Copper*; Karlin, K. D., Tyekler, J., Eds.; Chapman and Hall: New York, 1993. (c) Solomon, E. I.; Lowery, M. D.; Root, D. E.; Hemming, I. In *Mechanistic Bioinorganic Chemistry*; Thorp, H. H., Pecoraro, V. L., Eds.; American Chemical Society: Washington, DC, 1995; pp 121−164.

(3) (a) Casellato, V.; Vigato, P. A.; Fenton, D. E.; Vidali, M. *Chem. Soc. Rev.* **1979**, 8, 199. (b) Sorrell, T. N. *Tetrahedron* **1989**, *45*, 3. (c) Vigato, P. A.; Tamburini, S. *Coord. Chem. Rev.* **1990**, *106*, 25. (d) Zanello, P.; Tamburini, S.; Vigato, P. A.; Mazzocchin, G. A. *Coord. Chem. Rev.* **1987**, *77*, 165.

(4) (a) *Magneto-Structural Correlations in Exchanged Coupled Systems*; Willett, D. D., Gatteschi, D., Kahn, O., Eds.; NATO-ASI Series; Reidel: Amsterdam, 1985. (b) Kahn, O. *Molecular Magnetism*; VCH: New York, 1993.

S0020-1669(97)01495-X CCC: \$15.00

Chart 1

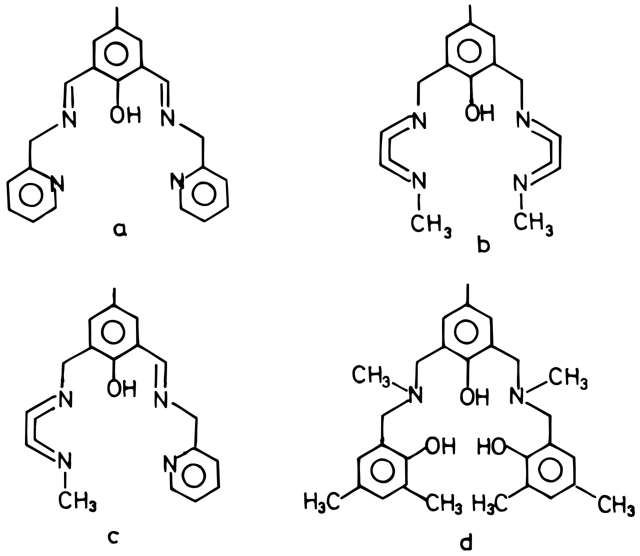

diformyphenols[5] (Chart 1a), *p*-substituted phenols[6] (Chart 1b), or substituted salicylaldehyde[7] (Chart 1c) with various primary and secondary amines. In all these cases, the imino or the amino nitrogens usually have no substituents or have hydrogen as the substituent. In contrast, the ligands H_3L^1 and H_3L^2 reported in the present work were obtained by the aminoalkylation of *p*-substituted phenols using 3,4-dihydro-3,6,8-trimethyl-2*H*-1,3-benzoxazine and 2-cyclohexylaminomethyl-4,6-dichlorophenol, respectively. In these ligands, the amino nitrogens have methyl or cyclohexyl substituents (Chart 1d).

As a continuation of our earlier work on binuclear copper(II) complexes,[8] we here report the synthesis and X-ray structural, spectral, electrochemical, and magnetic behavior of new binuclear copper(II) complexes derived from the ligands H_3L^1 and H_3L^2.

Experimental Section

Physical Measurements. Elemental analyses for the ligands and complexes were obtained on a Carlo Erba model 1106 elemental analyzer. ^{1}H NMR spectra (90 MHz) of the ligands were recorded using an FX-80Q Fourier transform NMR spectrometer, ^{13}C NMR spectra (100 MHz) of the ligands were recorded on a JEOL model GSX 400 NMR spectrometer, and the EI mass spectrum of the ligand H_3L^1 was recorded on a JMS-DX303 HF mass spectrometer. FAB mass spectra of the ligand H_3L^2 and complexes were recorded on an SX 102/DA-6000 mass spectrometer using 3-nitrobenzyl alcohol as the matrix solvent. IR spectra were recorded on a Hitachi 270-50 spectrophotometer on KBr disks in the range 4000−250 cm^{-1}. Electronic spectra were recorded on a Hewlett-Packard 8452A spectrophotometer in the range 250−820 nm. For cyclic voltammetry, a three-electrode system was used, in which the counter and working electrodes were platinum foils and the reference electrode was a saturated calomel electrode. The cyclic voltammograms were obtained on an apparatus comprising a PAR model 173 potentiostat/galvanostat, model 175 universal programmer, model 176 current/voltage converter, and model 179 coulometer and a Perkin-Elmer Hitachi 057 X-Y recorder. The measurements were carried out in dmf under oxygen-free conditions. Variable-temperature magnetic studies were performed on a PAR model 155 vibrating-sample magnetometer in the temperature range 77−300 K, and the instrument was calibrated using metallic nickel supplied with the instrument.

Materials. Tetraethylammonium perchlorate was purchased from Fluka and recrystallized from a methanol−water mixture. (***Caution!*** TBAP is potentially explosive; hence, care should be taken in the handling of this compound.) HPLC grade dimethylformamide was obtained from Qualigens's fine chemicals. The benzoxazine 3,4-dihydro-3,6,8-trimethyl-2*H*-1,3-benzoxazine[9] and the free Mannich base 2-cyclohexylaminomethyl-4,6-dichlorophenol[10] were prepared by following literature procedures. All other chemicals and reagents were of analytical grade and were used as without any further purifications.

Synthesis of the Ligands. The ligands H_3L^1 and H_3L^2 were synthesized by a single-step procedure as illustrated in Figure 1.

2,6-Bis[*N*−(3,5-dimethyl-2-hydroxybenzyl)-*N*-methylaminomethyl]-4-chlorophenol (H_3L^1). 3,4-Dihydro-3,6,8-trimethyl-2*H*-1,3-benzoxazine (8.85 g, 0.05 mol) and 4-chlorophenol (2.60 cm^3, 0.025 mol) were mixed by slight warming, and the mixture was kept stoppered at room temperature (30 °C). After 7 days, the viscous mass was diluted with 150 cm^3 of distilled methanol, and the mixture was kept at room temperature for 24 h. The colorless solid that precipitated was filtered off, washed with ice-cold methanol, and recrystallized from a benzene−methanol (1:1) mixture. Mp: 98 °C. Yield: 4.2 g (47%). ^{1}H NMR (CDCl$_3$/90 MHz/TMS): $\delta = 2.2$ (two close peaks, 18H), 3.6 (s, 8H), 6.7−7.1 (m, 6H). ^{13}C NMR (CDCl$_3$/100 MHz/TMS): $\delta = 15.9$, 20.3, 40.6, 58.7, 59.7, 122.3, 122.6, 124.3, 124.6, 128.1, 128.2, 128.7, 130.8, 152.1, 155.5. Mass (EI): *m/z* = 484 (M + 2). Anal. Calcd for $C_{28}H_{35}ClN_2O_3$: C, 69.71; H, 7.26; N, 5.81. Found: C, 70.35; H, 7.04; N, 5.96.

2,6-Bis[*N*-(3,5-dichloro-2-hydroxybenzyl)-*N*-cyclohexylaminomethyl]-4-methylphenol (H_3L^2). Paraformaldehyde (1.80 g, 0.06 mol) was taken in 75 mL of glacial acetic acid, 2-cyclohexylaminomethyl-4,6-dichlorophenol (13.61 g, 0.05 mol) was added, and the mixture was stirred at room temperature for 24 h. Then 4-methylphenol (2.60 mL, 0.025 mol) was added, and the mixture was stirred for 72 h. The resulting solution was heated on a water bath for 5 h, and the acid was neutralized with solid Na_2CO_3. The residue was extracted with CH_2Cl_2 (3 × 75 mL). A small amount of monoaminoalkylated phenol present in the dichloromethane extract, which is insoluble in a 90% dichloromethane−methanol mixture, was removed by filtration after the addition of 30 mL of methanol to the extract. The solvent was completely evaporated, and the residue was dissolved in 75 mL of 1-butanol. The light yellow solid that formed on slow evaporation of the solvent at room temperature for several days was filtered off and recrystallized from a CHCl$_3$−methanol (3:1) mixture. Mp: 120 °C. Yield: 5.3 g (34%). ^{1}H NMR (CDCl$_3$/90 MHz/TMS): $\delta = 1-2$ (two broad multiplets, 20H), 2.2 (s, 3H), 2.5 (br, 2H), 3.6 (s, 4H), 3.7 (s, 4H), 6.6−7.1 (m, 6H). ^{13}C NMR (CDCl$_3$/100 MHz/TMS): $\delta = 20.4$, 25.7, 26.0, 27.5, 50.7, 51.4, 59.1, 121.5, 122.1, 123.1, 125.8, 127.9, 128.0, 128.0 (two peaks merged), 130.1, 152.0, 154.2. Mass (FAB): *m/z* 680 (M + 2). Anal. Calcd for $C_{35}H_{42}Cl_4N_2O_3$: C, 61.76; H, 6.18; N, 4.12. Found: C, 62.26; H, 6.34; N, 4.28.

Binuclear Copper(II) Complexes of H_3L^1 and H_3L^2. [Cu_2L^1(OMe)]·MeOH (1). To a hot methanolic solution (50 mL) of the ligand H_3L^1 (0.48 g, 1 mmol) was added copper(II) acetate monohydrate (0.39 g, 2 mmol) dissolved in a minimum amount of water (5 mL). The crystalline solid that appeared within a few minutes was filtered off, washed with a little diethyl ether, and dried under vacuum. Crystals suitable for an X-ray crystallographic study were obtained by slow diffusion of diethyl ether through a dimethylformamide−methanol solution of the complex. Anal. Calcd for $C_{30}H_{39}ClCu_2N_2O_5$: C, 53.77; H, 5.83; N, 4.18. Found: C, 54.26; H, 5.95; N, 4.28.

The complexes **[Cu_2L^1(OH)] (2)** and **[Cu_2L^1Br] (3)** were prepared by the following general procedure. The ligand H_3L^1 (0.48 g, 1 mmol) in 50 mL of distilled methanol was first ionized with KOH (4 mmol),

---

[5] Robson, R. *Aust. J. Chem.* **1970**, *23*, 2217.

[6] Bertoncello, K.; Fallon, G. D.; Hodgkin, J. H.; Murray, K. S. *Inorg. Chem.* **1988**, *27*, 4750.

[7] Karlin, K. D.; Fenton, D. E.; Latour, J. M.; Smith, A. J. *J. Chem. Soc., Dalton Trans.* **1991**, 2979.

[8] (a) Karunakaran, S.; Kandaswamy, M. *J. Chem. Soc., Dalton Trans.* **1994**, 1595. (b) Karunakaran, S.; Kandaswamy, M. *J. Chem. Soc., Dalton Trans.* **1995**, 1851.

[9] Bruke, W. J.; Bishop, J. L.; Mortensen Glennie, E. L.; Bauer, W. N., Jr. *J. Org. Chem.* **1965**, *30*, 3423.

[10] Bruke, W. J.; Glennie, E. L. M.; Weatherbee, C. *J. Org. Chem.* **1964**, *29*, 909.

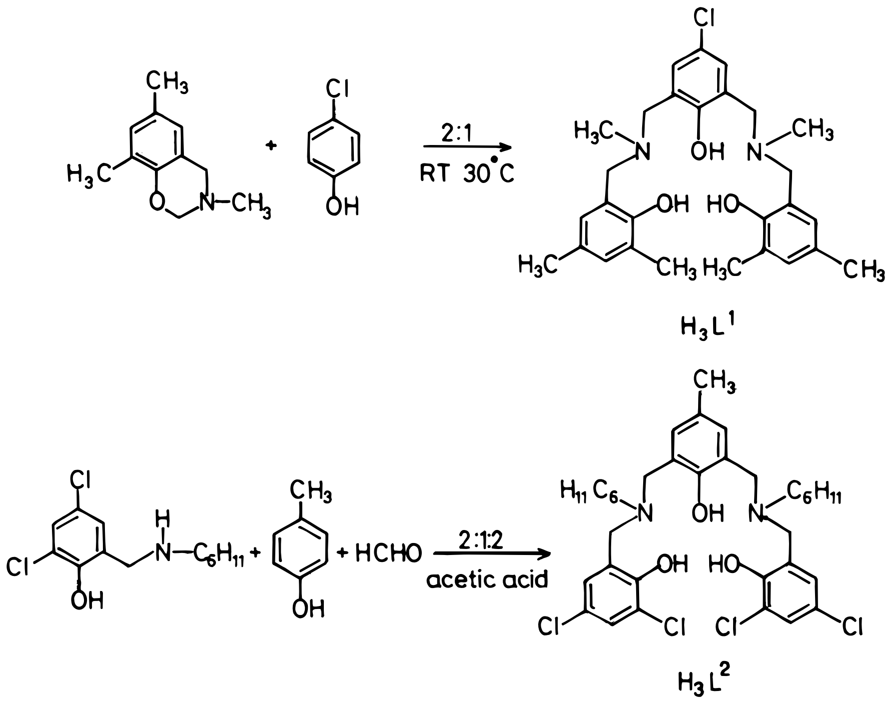

Figure 1. Schematic diagram for the syntheses of the ligands.

and this solution was added to the appropriate copper(II) salt (perchlorate and bromide, respectively, 2 mmol) dissolved in 25 mL of methanol. The resulting solution was refluxed on a water bath for 2 h. The solid that appeared on evaporation of the solvent was filtered off, washed with water, followed by little diethyl ether, and dried under vacuum. Anal. Calcd for **2**, $C_{28}H_{33}ClCu_2N_2O_4$: C, 53.89; H, 5.29; N, 4.49. Found: C, 54.25; H, 5.36; N, 4.71. Calcd for **3**, $C_{28}H_{32}BrClCu_2N_2O_3$: C, 48.95; H, 4.66; N, 4.02. Found: C, 48.83; H, 4.72; N, 4.26.

[Cu$_2$L^2(OMe)]·MeOH (4). To a hot methanol−dichloromethane (2:1, 40:20 v/v) solution of the ligand H_3L^2 (0.68 g, 1 mmol) was added copper(II) acetate monohydrate (0.39 g, 2 mmol) dissolved in minimum amount of water (5 mL), and the mixture was refluxed on a water bath for 15 min. The dark green crystalline solid that precipitated on standing at room temperature was filtered off, washed with a little diethyl ether, and dried under vacuum. Anal. Calcd for $C_{37}H_{46}Cl_4Cu_2N_2O_5$: C, 51.21; H, 5.30; N, 3.23. Found: C, 51.43; H, 5.52; N, 3.26.

The complexes **[Cu$_2$L^2(OH)] (5)** and **[Cu$_2$L^{2}Br] (6)** were prepared by following the general procedure adopted for the preparation of the complexes **2** and **3**. The ligand H_3L^2 (0.68 g, 1 mmol) in 50 mL of distilled methanol was first ionized with KOH (4 mmol), and this solution was added to the appropriate copper(II) salt (perchlorate and bromide, respectively, 2 mmol) dissolved in 25 mL of methanol. The resulting solution was refluxed on a water bath for 2 h. The solid that appeared on evaporation of the solvent was filtered off, washed with water followed by a little diethyl ether, and dried under vacuum. Anal. Calcd for **5**, $C_{35}H_{40}Cl_4Cu_2N_2O_4$: C, 51.28; H, 4.88; N, 3.42. Found: C, 51.52; H, 5.19; N, 3.69. Calcd for **6**, $C_{35}H_{39}BrCl_4Cu_2N_2O_3$: C, 47.67; H, 4.43; N, 3.18. Found: C, 47.61; H, 4.47; N, 3.47.

Crystal Structure Determination of [Cu$_2$L^1(OMe)]·MeOH. A dark green crystal of the copper(II) complex and methanol solvent having the approximate dimensions 0.30 × 0.20 × 0.10 mm was sealed in a glass capillary, and intensity data were measured at room temperature (294 K) on an Enraf-Nonius[11] CAD4 diffractometer equipped with graphite-monochromated Mo Kα ($\lambda = 0.710\,73$ Å) radiation using a variable-speed $\omega/2\theta$ scan technique. Cell dimensions and an orientation matrix for data collection were obtained from 25 high-angle reflections in the range $13 < \theta < 22°$. The octant measured was *hkl* ($0 \rightarrow 14$, $0 \rightarrow 17$, $-15 \rightarrow 15$). Three standard intensity-control reflections were recorded during every 60 min of X-ray exposure time. During the data collection, the intensity of the standard reflections decreased by 0.1%. A total of 4574 unique reflections were collected; of these, 2341 reflections had $F_o > 2.0$ and were used in the structure analysis. Data were corrected for Lorentz−polarization and absorption effects but not for extinction. The linear absorbance coefficient, μ, for Mo Kα radiation was 15.6 cm^{-1}.

The trial structure was obtained by direct methods using SHELXS-86[12] and refined by using MolEN.[13] The best *E* map revealed the positions of all the non-hydrogen atoms and one molecule of methanol solvent. Non-hydrogen atoms were refined anisotropically. Hydrogen atoms were located from successive difference Fourier maps and refined anisotropically. The final *R*-factor converged to 0.063 and $R' = 0.064$. Neutral-atom scattering factors were taken from Cromer and Waber.[14] During the refinement, the function minimized was $\sum w(|F_o| - |F_c|)^2$ with $w = 4F_o^2/[(\alpha(F_o^2)^2 + (0.04F_o^2)^2]$. The final Fourier map was featureless, with residual electron density values of ±0.49 e Å^{-3}. Anomalous dispersion effects were included in the final calculations;[15] the atomic scattering factors were taken from ref 14, and the mass attenuation coefficients were taken from ref 15. All calculations were performed on a MicroVax 3100 computer using CAD4 software. Data collection parameters and details of the structure solution and refinement are given in Table 1.

Results and Discussion

Structure of [Cu$_2$L^1(OMe)]·MeOH (1). The molecular structure of the binuclear complex [Cu$_2$L^1(OMe)]·MeOH along with the atomic labeling is given in Figure 2, and selected bond lengths and bond angles are summarized in Table 2. The ligand in the binuclear copper complex is pentadentate, each copper atom in the complex is tetracoordinated, and the geometry

---

[11] *CAD4 Software*, Version 5.0; Enraf-Nonius: Delft, The Netherlands, 1989.

[12] Sheldrick, G. M. *SHELXS-86: Program for the Solution of Crystal Structures*; University of Göttingen: Göttingen, Germany, 1986.

[13] Fair, C. K. *MolEN: An Interactive Intelligent System for Crystal Structure Analysis*; Enraf-Nonius: Delft, The Netherlands, 1990.

[14] Cromer, D. T.; Waber, J. T. *International Tables for X-ray Crystallography*; Kynoch Press: Birmingham, U.K., 1974; Vol. 4.

[15] Creagh, D. C.; McAuley, W. J. In *International Tables for X-ray Crystallography*; Wilson, A. J. C., Ed.; Kluwer: Boston, MA, 1992; p 219.

Table 1. Summary of Crystallographic Data for Complex 1

empirical formula	$C_{29}H_{35}N_2O_4Cu_2Cl\cdot MeOH$
fw	669.16
cryst size, mm	0.30 × 0.30 × 0.10
temp, K	293
space group	$P2_1/c$
a, Å	13.222(1)
b, Å	15.912(1)
c, Å	14.149(1)
β, deg	91.64(1)
V, Å^3	2975.47(6)
Z	4
d(calcd), Mg/m^3	1.487
$R(F_o)$[a]	0.063
$R'(F_o)$[b]	0.064
radiation/wavelength, Å	Mo Kα/0.710 73
μ(Mo Kα), cm^{-1}	15.62

[a] $R(F_o) = (\sum||F_o| - |F_c||)/(\sum|F_o|)$. [b] $R'(F_o) = (\sum w^{1/2}||F_o| - |F_c||)/(\sum w^{1/2}|F_o|)$; $w = 4F_o^2/[\sigma(F_o^2)^2 + (0.04F_o^2)]^2$.

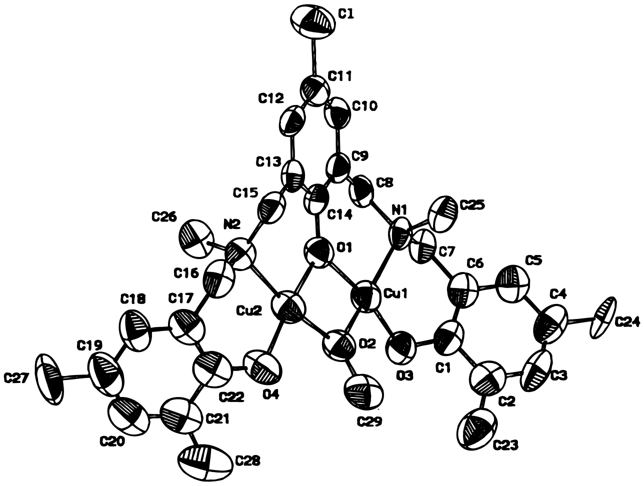

Figure 2. Molecular structure of $[Cu_2L^1(OMe)]\cdot MeOH$ showing the atomic labeling scheme. All hydrogen atoms have been omitted for clarity (50% probability thermal ellipsoids).

Table 2. Selected Bond Distances (Å) and Angles (deg) for **1**[a]

Cu1−O1	1.979(5)	O2−C29	1.41(1)
Cu1−O2	1.922(5)	O3−Cl	1.34(1)
Cu1−O3	1.888(6)	O4−C22	1.32(1)
Cu1−N1	1.992(6)	O5−C30	1.40(1)
Cu2−O1	1.973(5)	N1−C7	1.50(1)
Cu2−O2	1.892(6)	N1−C8	1.48(1)
Cu2−O4	1.888(6)	N1−C25	1.47(1)
Cu2−N2	1.999(6)	N2−C15	1.46(1)
Cl−C11	1.750(8)	N2−C16	1.51(1)
O1−C14	1.349(9)	N2−C26	1.47(1)
O1−Cu1−O2	76.6(2)	Cu1−N1−C25	110.5(5)
O1−Cu1−O3	169.6(2)	C7−N1−C8	104.9(6)
O1−Cu1−N1	92.0(2)	C7−N1−C25	109.6(6)
O2−Cu1−O3	95.8(2)	C8−N1−C25	110.6(6)
O2−Cu1−N1	160.8(2)	Cu2−N2−C15	107.8(5)
O3−Cu1−N1	97.1(2)	Cu2−N2−C16	107.1(5)
O1−Cu2−O2	77.5(2)	Cu2−N2−C26	113.4(5)
O1−Cu2−O4	170.4(2)	C15−N2−C16	108.6(6)
O1−Cu2−N2	91.3(2)	C15−N2−C26	110.9(6)
O2−Cu2−O4	94.0(2)	C16−N2−C26	108.8(6)
O2−Cu2−N2	168.7(2)	O3−C1−C2	118.8(7)
O4−Cu2−N2	97.3(3)	O3−C1−C6	123.9(8)
Cu1−O1−Cu2	100.1(2)	Cu1−O1−C14	130.2(5)
Cu2−O1−C14	128.4(5)	Cu1−O2−Cu2	105.2(5)
Cu1−O2−C29	127.0(5)	Cu2−O2−C29	124.2(5)
Cu1−O3−C1	120.2(5)	Cu2−O4−C22	120.1(5)
Cu1−N1−C7	110.8(4)	Cu1−N1−C8	110.3(4)
N2−C15−C13	116.1(6)	N1−C7−C6	112.7(6)
N2−C16−C17	114.1(7)	N1−C8−C9	114.0(6)

[a] Numbers in parentheses are estimated standard deviations in the least significant digits.

around the copper nuclei is best described as distorted square planar. The copper nuclei are bridged by a phenoxy oxygen atom provided by the central phenolic residue of the ligand in a symmetrical manner, resulting in comparable bond distances of Cu1−O1 = 1.979(5) Å and Cu2−O1 = 1.973(5) Å. These bond lengths are in good agreement with those observed in other μ-phenoxo-bridged bicopper complexes.[16] In addition, there is one more bridge between the two copper atoms formed by the exogenous methoxy group. This bridge is slightly asymmetric, with bond distances of Cu1−O2 = 1.922(5) Å and Cu2−O2 = 1.842(6) Å. The Cu1−O1−Cu2 bond angle is 100.1(2)° and Cu1−O2−Cu2 bond angle is 105.2(5)°, leading to a Cu1−Cu2 distance of 3.030(1) Å, which is normal for μ-phenoxo−μ-methoxo bridged complexes.[17] The coordination sphere is completed by one nitrogen and terminal phenoxide coordination of the ligand. The Cu−N and Cu−O bond lengths are in the regions of 1.992(6) and 1.888(6) Å, respectively, which are normal for planar copper(II) complexes.[18] The resulting structure around each copper is distorted square planar, and the four atoms Cu1, Cu2, O1, and O2 are in the same plane with a maximal deviation of 0.0858(5) Å from the mean plane. The dihedral angle between the two copper planes in the complex is 9.1(2)°. The methanol molecule found in the crystal is not coordinated to any of the copper atoms, and it occupies the crystal lattice as a free molecule.

Spectroscopy. The positive-ion FAB mass spectral study of complexes **2**, **4**, and **6** shows the molecular ion peak at m/z = 624 (10%) for **2**, 835 (25%) for **4**, and 884 (10%) for **6**, confirming the presence of a bicopper core in the complexes. The IR spectra of methoxy-bridged complexes **1** and **4** show nearly identical patterns. Both complexes show a sharp peak at 2805 cm^{-1}, which is assigned to the symmetrical C−H stretching vibration of the methoxy group.[19] The absence of a characteristic peak at 1520 cm^{-1} for the acetato group in both spectra indicates the absence of this group in these complexes. A characteristic peak for the OH group was observed at 3300 cm^{-1} for complexes **2** and **5**. The characteristic Cu−O, Cu−N, and Cu−Br vibrations for the complexes were observed as sharp peaks in the regions 475, 270, and 290 cm^{-1}, respectively. Electronic spectra of the complexes were recorded in dmf, and the data are summarized in Table 3. The absorption spectra of all the complexes exhibit three main features, one or two intense peaks below 300 nm assigned to the intraligand charge-transfer transitions ($\epsilon \approx$ 20 000 dm^3 M^{-1} cm^{-1}), a peak or shoulder in the range 390−430 nm due to phenolate to copper charge-transfer transitions ($\epsilon \approx$ 1000 dm^3 M^{-1} cm^{-1}), and a weak band around 650 nm ($\epsilon \approx$ 200 dm^3 M^{-1} cm^{-1}) for the usual copper d−d transition.[20] For square planar complexes, the d−d band

---

(16) Lubben, M.; Hage, R.; Meetsma, A.; Byma, K.; Feringa, B. L. *Inorg. Chem.* **1995**, *34*, 2217.

(17) (a) Karlin, K. D.; Dahlstrom, P. L.; Cozzette, S. N.; Scensny, P. M.; Zubieta, J. *J. Chem. Soc., Chem. Commun.* **1981**, 881. (b) Karlin, K. D.; Hayes, J. C.; Hutchinson, J. P.; Zubieta, J. *J. Chem. Soc., Chem. Commun.* **1983**, 376.

(18) O'Connor, C. J.; Firmin, D.; Pant, A. K.; Babu, P. R.; Stevens, E. D. *Inorg. Chem.* **1986**, *25*, 2300.

(19) Crane, D.; Fenton, D. E.; Latour, J. M.; Smith, A. J. *J. Chem. Soc., Dalton Trans.* **1991**, 2979.

(20) (a) Karlin, K. D.; Cohenn, I.; Hayes, J. C.; Farooq, A.; Zubieta, J. *Inorg. Chem.* **1987,** *26*, 147. (b) Hathway, B. J. In *Comprehensive Coordination Chemistry*; Wilkinson, G., Ed.; Pergamon: New York, 1987; Vol. 5, p 533.

Table 3. Electronic Spectral Data for the Complexes: λ_{max}/nm (ϵ/dm^3 mol^{-1} cm^{-1})

no.	complex	d−d	CT[a]
1	[Cu$_2$L^1(OMe)]·MeOH	638 (328)	408 (sh), 273 (17 441), 266 (15 649)
2	[Cu$_2$L^1(OH)]	667 (196)	398 (sh), 288 (14 965), 268 (17 650)
3	[Cu$_2$L^{1}Br]	666 (362)	380 (1935), 285 (10 020)
4	[Cu$_2$L^2(OMe)]	647 (281)	396 (sh), 298 (16 530)
5	[Cu$_2$L^2(OH)]	698 (267)	410 (sh), 320 (26 315)
6	[Cu$_2$L^{2}Br]	675 (104)	420 (666), 298 (18 988)

[a] CT = charge transfer band. sh = shoulder.

is usually observed in the region 600−650 nm. The complexes reported in the present work show the d−d band in the region 630−700 nm, and this red shift may be due to the distortion from square planar geometry.[21] The red shift in the λ_{max} value of the d−d band observed for the complexes of the ligand H$_3$L^2 when compared to the complexes of the ligand H$_3$L^1 indicates that the coordination geometry of the former complexes is more distorted than that of the latter complexes.

Electrochemistry. Reduction at negative potentials is the usual trend observed for phenoxo-bridged binuclear copper complexes and is likely the result of the "hard" nature and negative influence[22,23] of the phenoxide ligand.

Electrochemical behavior of the complexes reported in the present work was studied by cyclic voltammetry in the potential range 0 to −1.4 V in dimethylformamide containing 0.1 M tetraethylammonium perchlorate, and the data are summarized in Table 4. The cyclic voltammograms for complexes **1** and **5** are depicted in Figure 3. Each voltammogram shows two well-defined quasireversible reduction steps at negative potentials. Controlled-potential electrolysis carried out for complexes **1** and **5** at 100 mV more negative than the first reduction step consumed one electron per molecule ($n = 0.95$) and at 100 mV more negative than the second reduction step consumed two electrons per molecule ($n = 1.93$) (−2 F/mol). These results indicate that the two reduction peaks are associated with the stepwise reduction of the copper(II) center

$$\mathrm{Cu^{II}Cu^{II}} \xrightarrow{E^1_{pc}} \mathrm{Cu^{II}Cu^{I}} \xrightarrow{E^2_{pc}} \mathrm{Cu^{I}Cu^{I}}$$

and the conproportionation constant for the equilibrium

$$\mathrm{Cu^{II}Cu^{II}} + \mathrm{Cu^{I}Cu^{I}} \overset{K_{con}}{\rightleftharpoons} 2\mathrm{Cu^{II}Cu^{I}}$$

was calculated using the relationship $\log K_{con} = \Delta E/0.0591$.[24]

From Table 4 it is seen that complexes **4**−**6** of the ligand H$_3$L^2 undergo reduction at less negative potential (−0.37 to −0.45 V) relative to complexes **1**−**3** of the ligand H$_3$L^1 (−0.61 to −0.68 V). The less negative reduction potential observed for complexes **4**−**6** can be explained on the basis of the substitutional steric and electronic effects of the ligand H$_3$L^2. Both electronic and steric effects of the bulky cyclohexyl group would play a significant role in determining the reduction potential. Since methylamine is more basic than the cyclohexylamine[25a] of the ligand H$_3$L^2, the former would be a good electron donor compared to the latter and the bulky cyclohexyl group of the ligand H$_3$L^2 would likely effect a distorted geometry[25b] for the copper atoms in complexes **4**−**6**. Further, the electron-withdrawing chlorine atoms positioned on the terminal phenolic residues decrease the electron density on the copper atoms[26] of the complexes derived from the ligand H$_3$L^2. All these factors, in the complexes of the ligand H$_3$L^2, would destabilize the copper(II) oxidation state by reducing the electron density on the copper atoms and by providing a distorted coordination geometry for the copper atoms, consequently influencing the reduction at less negative potential relative to that for the complexes of H$_3$L^1.

A comparison of the electrochemical data of the complexes of the ligand H$_3$L^1 or H$_3$L^2 indicates that the reduction potential for the methoxy-bridged complex **1** is more negative (−0.68 V) than that for the hydroxo-bridged complex **2** (−0.66 V), which is in turn more negative than that for the bromo-bridged complex **3** (−0.61). This behavior may be due to reduction in electron density on the copper atoms as a result of the decreasing electron-donating ability of the exogenous donor atoms in the following order: OMe > OH > Br. For both bromo-bridged complexes **3** and **6**, the shift in the reduction potential toward less negative potential is more pronounced. This behavior may be due to the combination of effects due to the lesser electron-donating nature of the bromide ion and distortion in the coordination geometry induced by the relatively bulky bromide ion[18] in these complexes.

It is of interest to compare the electrochemical behavior of the complexes **1**−**6** with that of **1a** (Chart 2), whose electrochemistry has been studied[27] extensively. Under the same electrochemical conditions (20 °C, dmf, TEAP, Pt electrode, scan rate 100 mV/s), **1a** has shown a completely reversible first reduction at −0.850 V and a quasireversible second reduction at −1.230 V. In contrast, complexes **1**−**6** undergo irreversible or quasireversible reduction at less negative potentials, indicating the easy reduction of the complexes **1**−**6** at the electrode surface. This behavior is attributable to the restricted free rotation of the C═N bond of complex **1a** when compared to the flexible C−N bond in the complexes of the ligands reported in the present work and to the steric effects[28,29] of the bulky alkyl substituents on nitrogen and at the remote environments of the ligands. All these factors would facilitate Cu(II) → Cu(I) reduction at less negative potential. The peak separation observed for the complexes **1**−**6** is less when compared to that for complex **1a**, indicating that the mixed-valent species formed as a result of the reduction of complexes **1**−**6** were less stable than that formed by the reduction of **1a**. This behavior is likely due to the unsaturated nature of the ligand of **1a**. In the case of unsaturated binuclear copper(II) complexes, stepwise saturation of the azomethine linkage by donation of electrons from the filled d orbital of the Cu(I) through the antibonding orbital of the C═N linkage results in larger peak separation between the reduction waves, in accordance with the results observed

---

[21] Bhalla, R.; Helliwell, M.; Garner, C. D. *Inorg. Chem.* **1997**, *36*, 2944.

[22] (a) Patterson, G. S.; Holm, R. H. *Bioinorg. Chem.* **1975**, *4*, 257. (b) Karlin, K. D.; Gultnech, Y. *Prog. Inorg. Chem.* **1987**, *35*, 219.

[23] Benzekeri, A.; Dubourdeaux, P.; Latour, J. M.; Rey, P.; Laugier, J. *J. Chem. Soc., Dalton Trans.* **1991**, 3359.

[24] (a) Gagne, R. R.; Koval, C. A.; Smith, T. J. *J. Am. Chem. Soc.* **1977**, *99*, 8367. (b) Gagne, R. R.; Koval, C. A.; Smith, T. J.; Cimolino, M. C. *J. Am. Chem. Soc.* **1979**, *101*, 4571.

[25] (a) Roberts, J. D.; Chambers, V. C. *J. Am. Chem. Soc.* **1951**, *73*, 5030. (b) Chuang, C. L.; Lim, K.; Chen, Q.; Zubieta, J.; Canary, J. W. *Inorg. Chem.* **1995**, *34*, 2562.

[26] Zubieta, J.; Hayes, J. C.; Karlin, K. D. In *Copper Coordination Chemistry. Biochemical and Inorganic Perspectives*; Karlin, K. D., Zubieta, J., Eds.; Adenine: Guilderland, New York, 1983; p 97.

[27] Mazurek, W.; Bond, A. M.; Murray, K. S.; O'Conner, M. J.; Wedd, A. J. *Inorg. Chem.* **1985**, *24*, 2484.

[28] Domenech, L.; Jalgado, J. V.; Garcia-Espana, E.; Luis, S. V.; Lliuras, M.; Miravet, J. F.; Ramirez, J. A. *J. Chem. Soc., Dalton Trans.* **1995**, 541.

[29] (a) Gagne, R. R.; Koval, C. A.; Smith, T. J. *J. Am. Chem. Soc.* **1979**, *101*, 6921. (b) James, P. R.; Williams, R. J. P. *J. Chem. Soc.* **1961**, 2007.

Table 4. Electrochemical Data for the Complexes in dmf[a]

no.	complex	E^1_{pc}	E^1_{pa}	$E_{1/2}$ (ΔE/mV)	E^2_{pc}	E^2_{pa}	$E_{1/2}$ (ΔE/mV)	K_{con}
1	$[Cu_2L^1(OMe)]\cdot MeOH$	−0.68	−0.48	−0.58 (200)	−0.91			
2	$[Cu_2L^1(OH)]$	−0.66	−0.39	−0.53 (270)	−0.85			
3	$[Cu_2L^1Br]$	−0.61	−0.25	−0.43 (360)	−0.88	−0.42	−0.65 (460)	5.27×10^3
4	$[Cu_2L^2(OMe)]$	−0.45			−0.75	−0.53	−0.64 (220)	
5	$[Cu_2L^2(OH)]$	−0.43	−0.27	−0.35 (160)	−0.72	−0.48	−0.60 (240)	1.69×10^5
6	$[Cu_2L^2Br]$	−0.37	−0.18	−0.28 (190)	−0.71	−0.44	−0.58 (270)	1.19×10^4

[a] V vs SCE. Conditions: Pt working and SCE reference electrodes; supporting electrolyte TEAP; concentration of complex 1×10^{-3} M, concentration of TEAP 1×10^{-1} M.

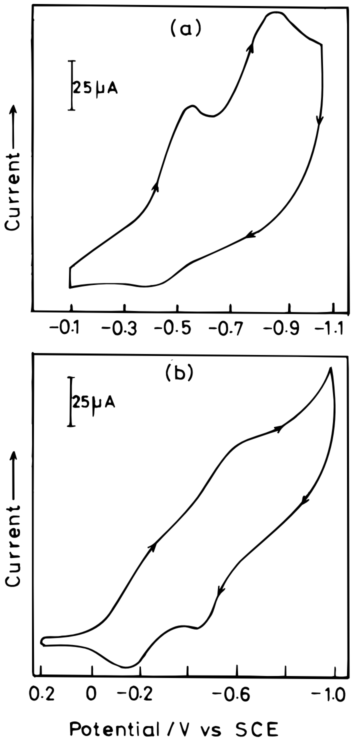

Figure 3. Cyclic voltammograms for (a) $[Cu_2L^1(OMe)]\cdot MeOH$ (**1**) and (b) $[Cu_2L^2(OH)]$ (**5**).

Chart 2

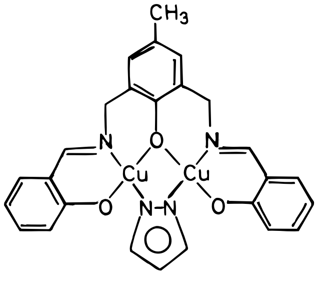

Table 5. Temperature Dependence of the Magnetic Parameters for the Complexes[a]

no.	complex	$-2J$, cm^{-1}	P	g	$10^{-3}[R(\chi)]$
1	$[Cu_2L^1(OMe)]\cdot MeOH$	299	0.10	2.1413	3.162
2	$[Cu_2L^1(OH)]$	258	0.12	2.2109	9.167
3	$[Cu_2L^1Br]$	176	0.22	2.2811	4.505
4	$[Cu_2L^2(OMe)]$	204	0.20	2.2009	4.644
5	$[Cu_2L^2(OH)]$	170	0.07	2.2341	6.944
6	$[Cu_2L^2Br]$	128	0.075	2.1201	4.206

[a] N_α has been fixed as 120×10^{-6} cm^3/mol for all magnetic simulations.

for some macrocyclic complexes.[30] In addition to all these contrasting behaviors, **1a** shows better electrochemical reversibility when compared to complexes **1**−**6**. This behavior may be due to the influence of the exogenous pyrazole coordination in complex **1a**, since reversibility of the irreversible electrochemical behavior has been observed for a hydroxo-bridged binuclear copper(II) complex upon simple replacement of the hydroxide by a pyrazole residue.[29a] Hence, in addition to the effect of the exogenous bridging entity, general reasons for an electrode process to be irreversible such as the inability of the complexes to adopt the required stereochemical changes, speedy chemical reactions followed by the reduction processes, removal of the exogenous ligand atom prior or subsequent to electron transfers, nonspecific interactions of solvent with species in different oxidation states, etc. are also responsible for the irreversible or quasireversible nature of the reduction processes in the present series of complexes.[31]

Magnetochemistry. Low magnetic moment values in the range 0.8−0.9 μ_B/Cu observed at room temperature for the complexes indicate the presence of a spin exchange interaction between the copper atoms. A variable-temperature magnetic study of complexes **1**−**6** was performed in the temperature range 77−300 K, and the experimental magnetic susceptibility values were fitted to the Bleany−Bowers equation[32] to evaluate the singlet−triplet energy separation ($-2J$):

$$\chi_m = (Ng^2\beta^2/3kT)[3 + \exp(-2J/kT)]^{-1}(1 - P) + N_\alpha$$

In this expression, χ_m is the molar magnetic susceptibility corrected for diamagnetism, P is the percentage of monomeric impurities, and other symbols have their usual meaning. $-2J$ values were evaluated by a nonlinear regression analysis in which $-2J$, P, and g are the variables. The parameters giving a best fit to the experimental susceptibility values are listed in Table 5. N_α has been fixed as 120×10^{-6} cm^3 M^{-1} for all magnetic simulations. A small discrepancy factor defined as $R(\chi) = \sum(\chi_{obsd} - \chi_{calcd})^2/\sum(\chi_{obsd})^2$ observed for the complexes indicates a good agreement between the observed and theoretical magnetic susceptibility values. Temperature dependence magnetic properties of complexes **1** and **5** are depicted in Figure 4.

Magneto−structural correlations for several hydroxo-,[33] alkoxo-,[34] and phenoxo-bridged[35] dicopper complexes show that

---

(30) (a) Mandal, S. K.; Thompson, L. K.; Nag, N.; Charland, J. P.; Gaba, E. J. *Inorg. Chem.* **1987**, *26*, 1391. (b) Berends, H. P.; Stephan, D. W. *Inorg. Chem.* **1987**, *26*, 749. (c) Long, R. C.; Hendrickson, D. N. *J. Am. Chem. Soc.* **1983**, *105*, 1513. (d) Okawa, H.; Tadokoro, M.; Aratake, Y.; Ohba, M.; Shindo, K.; Mitsumi, M.; Koikawa, M.; Tomono, M.; Fenton, D. E. *J. Chem. Soc., Dalton Trans.* **1993**, 253.

(31) Bailey, N. A.; Fenton, D. E.; Lay, L.; Roberts, P. R. *J. Chem. Soc., Dalton Trans.* **1986**, 2681.

(32) Bleaney, B.; Bowers, K. D. *Prog. R. Soc. London, Ser. A* **1952**, *214*, 415.

(33) Crawford, V. H.; Richardson, H. W.; Wasson, J. R.; Hodgson, D. H.; Hatfield, W. E. *Inorg. Chem.* **1976**, *15*, 5. 2107.

(34) Merz, L.; Hasse, W. *J. Chem. Soc., Dalton Trans.* **1980**, 875.

(35) Thompson, L. K.; Mandal, S. K.; Tandon, S. S.; Bridson, J. N.; Park, M. K. *Inorg. Chem.* **1996**, *35*, 3117.

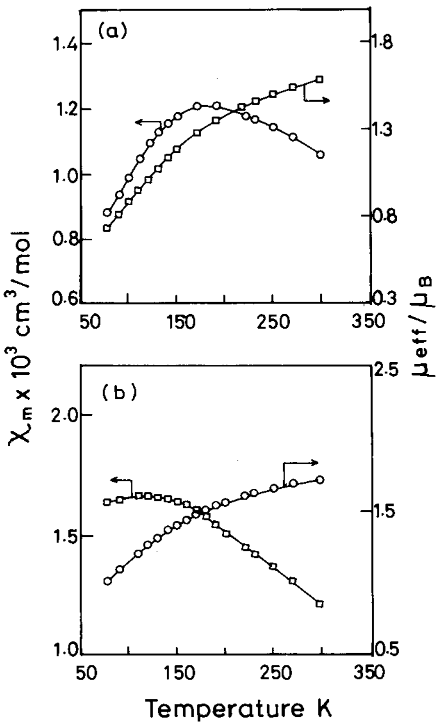

Figure 4. Temperature dependence of the magnetic properties of (a) $[Cu_2L^1(OMe)]\cdot MeOH$ (**1**) and (b) $[Cu_2L^2(OH)]$ (**5**).

the major factor controlling the exchange interactions is the Cu−O−Cu bridge angle; however, other factors such as electronegativity of the bridging atom, electronic perturbation by remote substituents, degree of distortion from planar geometry, and the dihedral angle between two copper planes also have considerable influence on the extent of spin−spin interaction.

With few exceptions,[16,19] magneto−structural correlations for several phenoxo-bridged dicopper complexes with $Cu-O_{ph}-Cu$ bridge angles greater than 99° generally show exchange coupling values greater than 420 cm^{-1}, and for the complexes with bridge angles less than 98°, the exchange interaction is less (<70 cm^{-1}).[36] For the complex $[Cu_2L^1(OMe)]\cdot MeOH$, the $Cu-O-Cu_{(Av)}$ bridge angle is 102.6° and the observed exchange interaction value is 299 cm^{-1}. The possible reason for the low $-2J$ value may the deviation from coplanarity within the central Cu_2O_2 moiety. The dihedral angle between the Cu(1)O(1)O(2) and Cu(2)O(1)O(2) planes is 9.1(2)°, and strong antiferromagnetic coupling is observed only in complexes in which the two planes are coincident.[16]

Since, the natures of the donor atoms and exogenous bridging groups in both types of the complexes are same, a comparison of the magnetic properties would be useful in discovering the possible substitutional effects on spin exchange interactions in the complexes. As observed in the electrochemical studies, here also a smaller $-2J$ value is observed for the complexes of the ligand H_3L^2 when compared to the complexes of the ligand H_3L^1, and this behavior can be explained on the basis of the distorted square planar geometry around the copper atoms as a result of the bulky cyclohexyl group and generation of considerable electropositive character on the copper atoms due the reduction of electron density by the electron-withdrawing effect of the chlorine atoms. Reports suggest that both distortion from planar geometry[35] and reduction in electron density on the copper atoms[37] are less favorable for effective spin exchange interactions, and hence smaller exchange integral values were observed for the complexes of the ligand H_3L^2 compared to the complexes of the ligand H_3L^1. For both types of complexes, within the series the observed $-2J$ value is greatest for the methoxo-bridged complex (299 cm^{-1} for **2**), less for the hydroxo-bridged complex (258 cm^{-1} for **2**), and further less for the bromo-bridged complex (176 cm^{-1} for **3**). Since, the electron-donating nature of the exogenous donor ligands follows the order OMe > OH > Br, the electron density on the copper atoms will decrease in the same order; consequently, the superexchange interaction decreases in the same order.[38]

In conclusion, it has been observed that the substitutional effects on the electrochemical and magnetic behaviors of the complexes derived from the ligands agree well with the established trend. The observed electrochemical and magnetic behaviors of the complexes have been explained on the basis of the steric effects and electronic perturbations due to the substituents located on the donor atoms and also at the peripheral region of the ligand environments.

Acknowledgment. We wish to thank Dr. P. Natarajan for his assistance in obtaining the elemental analysis data. L.G. and D.V. thank the CSIR, India, and P.A. thanks the UGC, India, for financial support.

Supporting Information Available: Tables of X-ray methods, atomic coordinates, bond distances and angles, thermal parameters, hydrogen atom positional parameters least-squares plane data, and H-bonding interactions for complex **1** (7 pages). Ordering information is given on any current masthead page.

IC9714955

---

(36) (a) Nishida, Y.; Shimo, H.; Maehara, H.; Kida, S. *J. Chem. Soc., Dalton Trans.* **1985**, 1945. (b) Sorrell, T. N.; Jameson, T. L.; O'Connor, C. J. *Inorg. Chem.* **1984**, *23*, 190. (c) Lorosch, L.; Hasse, W. *Inorg. Chim. Acta* **1985**, *108*, 35.

(37) Brichery, K.; Drager, K.; Jens, K. T.; Tilset, M.; Betrem, M. *Chem. Ber.* **1994**, *127*, 465.

(38) (a) Handa, M.; Koga, N.; Kida, S. *Bull. Chem. Soc. Jpn.* **1988**, *11*, 3853. (b) Astheimer, H.; Hasse, W. *J. Chem. Phys.* **1986**, *85*, 1427. (c) Galy, J.; Jaod, J.; Khan, O.; Dola, P. *Inorg. Chim. Acta* **1979**, *36*, 229.